University of Baghdad
College of Engineering
JOURNAL OF ENGINEERING

Journal of Engineering

journal homepage: www.jcoeng.edu.iq

Volume 30 Number 5 May 2024

Adaptive Pixel-Based Technique for Grayscale Image Compression

Zahraa.H. Abed[1,*], Ghadah K. AL-Khafaji[2]

Department of Computer Science, College of Science, University of Baghdad, Baghdad, Iraq
Zahraahusam83@gmail.com[1], ghada.toma@sc.uobaghdad.edu.iq[2]

ABSTRACT

Grayscale images are extensively used due to their simplicity and cheapness in storage and transmission compared to color one of RGB base. It can also be considered a solution for color-blind people to ensure a better view of things and reading. However, unfortunately, it is still quite overburdened with redundancy(s) in which the data compression exploits them efficiently depending on the type and way of redundancy removal. This work introduces a hybrid compression system to compress grayscale images using the adaptive pixel-based technique (PBT) of optimized modeling base, with incorporated Minimize Matrix Size Algorithm (MMSA) of three digits values (C321) to encode the residual compactly along the need to overhead information (index, mean). Adapting traditional PBT led to overcoming the problems in the conventional PBT system in terms of large size. It achieved an acceptable reduction in bytes for the deterministic part (*M, Indx*) of over 400 bytes and the deterministic part (Res), where the size was reduced to more than 5000 bytes on average. The size has been reduced by nearly 50% compared to traditional PBT. The tested results indicate higher quality compared to the standard JPEG and traditional PBT in terms of performance. This includes a Compression Ratio (CR) of 13 and a PSNR of 48 dB.

Keywords: Image Compression, Pixel-Based, JPEG, Limited Space Search Table, Support Data, Minimize Matrix Size Algorithm

*Corresponding author
Peer review under the responsibility of University of Baghdad.
https://doi.org/10.31026/j.eng.2024.05.04

Article received: 15/06/2023
Article accepted: 10/09/2023
Article published: 01/05/2024

طريقة مطورة لضغط الصور الرمادية القائمة على البكسل

زهراء حسام عبد*, غادة كاظم الخفاجي

قسم علوم الحاسوب، كلية العلوم، جامعة بغداد، بغداد، العراق

الخلاصة

يتم استخدام الصور ذات الدرجات الرمادية بشكل واسع , بسبب بساطتها ورخصها من حيث التخزين والنقل مقارنة بالصور الملونة المبنية على نظام *RGB* ، ويمكن اعتبارها حلاً للأشخاص الذين يعانون من عمى الألوان لضمان رؤية وقراءة أفضل للأشياء, ولكن للأسف لا تزال تحمل عبئًا زائدًا من التكرارات التي يتم استغلال ضغط البيانات لها بكفاءة وفقًا لنوع وطريقة إزالة التكرار. يقدم هذا العمل ، نظام ضغط هجين لضغط الصور الرمادية باستخدام تقنية القائم على البكسل مبنية على نمذجة محسّنة ، مع استخدام خوارزمية تصغير حجم المصفوفة *(MMSA)* مدمجة من ثلاثة أرقام *(C321)* لضغط *residual* مع الحاجة إلى المعلومات العامة (*index* ، *mean*). أدى تكيف نظام *PBT* التقليدي إلى التغلب على المشكلات التي حدثت في نظام *PBT* التقليدي من حيث الحجم الكبير. حقق انخفاضًا مقبولًا بالبايت للجزء *deterministic* (*M* , *Indx)* لأكثر من 400 بايت والجزء *deterministic (Res)* , حيث تم تقليل الحجم كمعدل يصل إلى أكثر من 5000 بايت. تم تقليل الحجم بنسبة 50% مقارنةً بـ *PBT* التقليدي. تشير النتائج المختبرة إلى جودة أعلى مقارنةً بتنسيق *JPEG* القياسي والتقنيات التقليدية القائمة على البكسل من حيث الأداء. يتضمن ذلك نسبة ضغط بلغت 13 و *PSNR* بلغت *48*.

الكلمات المفتاحية: ضغط الصور، القائمة على البكسل ,جدول البحث في مساحة محدودة , بيانات سانده , خوارزمية تصغير حجم المصفوفة

1. INTRODUCTION

The image is the foundation for various daily applications, including sharing personal photos, transmitting news, lectures, and medical images. However, a significant issue arises due to the large file sizes associated with these images, which can impact device storage and network bandwidth **(Salman and Rafea, 2020; Shihab, 2023; Mohammed et al., 2021)**. Image compression systems aim to address this problem by efficiently preserving image information while eliminating unnecessary redundancy found among neighboring pixels **(Abouali, 2013; Ahmed et al., 2020; Hussain et al., 2020; Ahmed et al., 2021**; **Mahdi and Al-khafaji, 2022)**. In addition, using Internet applications has become necessary, meaningful, and indispensable, as most things are currently managed via the Internet. Social media platforms enable people to communicate with each other easily, inexpensively, and instantly, exchanging ideas or content using devices such as smartphones, tablets, and computers. On these platforms, images play a vital role in news showcasing, entertainment, and events like Eid, Christmas, and birthdays, especially after COVID-19 **(Ibrahim et al., 2020; Abd-Alzhra and Al-Tamimi, 2022; ALKhafaji et al., 2023).** The need to use Internet applications has become necessary, important, and indispensable. Consequently, the process of data compression has become an urgent and essential process because large amounts of data are dealt with, whether in online buying and selling or through distance learning and

the use of social media between people **(Chuman, 2017; Maghari, 2019; George et al., 2020; Abd-Alzhra and Al-Tamimi, 2021)** Image compression compresses important and necessary information and reduces redundant, unimportant, and duplicate information from the image. Therefore, the main goal of image compression is to represent the image in the least possible bits without losing the content of the necessary and basic information within the scope of the original image **(Abood, 2013; Al-Khafaji and Fadhil, 2017; Rafea and Salman, 2018; Al-Khafaji and Gorrge, 2021)**. Compression techniques have been developed to overcome and address the challenges and problems that have emerged recently. In view of the increasing growth of technology, where huge amounts of data must be stored correctly using compression algorithms and in different ways, some of which are lossy or lossless **(Hussain et al., 2018; Ahmed et al., 2021; Salman, 2021; Yousif and Salman, 2021)**.

Recently developed techniques for efficient spatial coding removal Pixels-based compression techniques can be considered as an optimized Predictive Coding (PC)or Differential Pulse Code Modulation (DPCM) technique without converting them to the frequency domain to eliminate interpixel redundancy, utilizing the mean value and trying to identify the model of each pixel value corresponding to the best value of minimum residual **(Maksimov and Gashnikov, 2018; Kabir and Mondal, 2018; Abed and Al-khafaji, 2022)**. It incorporates the Minimize Matrix Size Algorithm (MMSA) to encode the residual of three-digit values (C321) compactly and efficiently. The technique enables the lossless representation of each set of three data values using a single floating-point value by utilizing weighted random values between [0-1] **(Siddeq and Rodrigues, 2015; Rasheed et al., 2020; Al-hadithy et al., 2021; Al-hadithy and Al-khafaji, 2022)**.

Sultan and George presented a lossy hybrid compression system that encodes the pixel-based modeling scheme of the deterministic part (mean, index) and probabilistic part (residual) separation into two parts: the Most Significant Value(MSV) and the Least Significant Value(LSV) using various techniques **(Sultan and George, 2021)**. These techniques include DPCM, Bit Plane Slicing (BPS), and C32 of MMSA, along with a three-lossless-values-based sequential search scheme with three keys of the logistic map. This approach is adopted instead of the traditional random key generator **(Pak and Huang, 2017; Ahmed and Hamza, 2021)**. Using the same keys throughout the MMSA process provides flexibility and avoids needing different randomly generated keys as in traditional techniques. The keys play a role in reducing the size and achieving higher compression ratios compared to the conventional approach. Support Data (SD) also speeds up the encoding and decoding processes. The combination of DWT hierarchical scheme and hard thresholding is suggested as an efficient coding technique, which leads to improved CR while preserving grayscale image quality.

This work aims to build an efficient grayscale compression system using a spatial domain of pixel-based coding techniques. This review section below concentrates on aspects relevant to the subjects of this work that are discussed separately. The first part is related to the work of pixel-based image compression, and the second part is related to the MMSA.

1.1 Pixel Base Technique

This subsection is devoted to reviewing details of (PBT) which can be considered as an extension optimized model of the PC techniques, such as:

(Azman et al., 2019) proposed a hybrid lossless grayscale image compression system that combined DPCM (third order, 2D structure, Casual model) with Haar DWT and entropy

coding of Huffman coding techniques. The system's performance is evaluated using five standardized grayscale square images (Lena, Baboon, Goldhill, Peppers, Cameraman) of square size 512 × 512 pixels. The highest CR value for Lena image equals to (1.5457), Baboon (1.0522), Goldhill (1.3181), Peppers (1.4644), and Cameraman (2.1214), the system unfortunately achieved low compression performance as spatial lossless techniques.

(Hussain and Al-Khafaji, 2021) introduced a new pixel-based compression technique of optimized minimum residual to compress grayscale images efficiently and lossily. The DWT of Haar base was utilized along the hierarchal quantization scheme to compress the residual and the lossless coding techniques used for the mean vector and indexes. The system was tested with three standard grayscale square images of size 256×256 (Cameraman, Girl, and Lena), with a different number of neighbors(ngb), increment values (inc =0.25, ngb=10, and inc=0.125, ngb=0.125), and hierarchal quantization steps values of Q (20 and 30), β(0.8-1.3), α(0.6-1.6), where CR exceeds 12 with excellent quality over 41dB, but unfortunately suffers from large residual error. **(Liu et al., 2022)** suggested a lossless image compression system that mixes linear (PC) and (IWT) that rounded the subbands values and neglected zeros/negative values (wavelet coefficients), followed by Huffman coding techniques. The performance of the proposed system has been tested on different images, sizes ranging from 256 ×256 to 512×512 pixels according to the Waterloo Image Compression Benchmark, which shows the bpp of the proposed algorithm with a range from (0.6989 to 5.1664). The problem with this work is the simplicity of an encoder that utilized Huffman coding only to eliminate details subband values.

1.2 Minimize Matrix Size Algorithm

This subsection is devoted to reviewing details relevant to MMSA and enhancements or improvements, such as:

(Siddeq and Al-Khafaji, 2013) proposed a simple lossy image compression scheme that is based on two transformation techniques in the frequency domain of DWT and DCT to decompose the image is parsed into subranges (LL, LH, HL, and HH), the approximate sub quadrants portion (LL) used is divided into no overlapping blocks of fixed size n×n, and performs the DCT. At the same time (LH, HL, and HH) contain very small details, which can be set to zero without much change to the image. Then using (MMSA) encodes the compressed information that reduces high-frequency matrix size efficiently and makes it easy to compress by arithmetic coding. The proposed system is evaluated using three square and non-square grayscale images (Lena, Iris, and X-ray), and experimental outcomes are assessed using weights (keys) of MMSA = 0.9133,0.1269,0.9057 and Quality values between [0.02- 0.05]. The CR for the Lena image size of 500×500 ranges from (12.5 to 19.2) with PSNR values ranging from 33.1dB to 32.1 dB. While CR for Iris images size of 512×512 ranges between (17.5 and 30.8) with PSNR values between 36.1 and 34.6 dB. Lastly, for the X-ray image size of 500×522, the CR was between (17.4 and 30.7), with PSNR values ranging from dB 30.1 to 29.6 dB. Compared to JPEG and JP2 standard procedures, JPEG2000 offers varied attributes to maintain image quality greater than the proposed method. **(Siddeq and Rodrigues, 2017)** suggested a lossy system compression that combines DCT and MMSA. Where the image is divided firstly into (non-fixed) blocks, and then the DCT exploits each block. After that, each block is converted into a 1D vector, removing the zero values from the AC coefficients.

In contrast, zero values are preserved where matrix minimization is applied to it to reduce each block by 2/3 and create a table to hold the probabilistic data to enable recovery of the

original high frequencies by searching this table to be used in the decompression phase and apply PC or delta operator to the vector of the DC-components. Finally, arithmetic coding is applied for DC and AC coefficients. The experimental results were tested using three standard 2D images (Apple, Face, and Ship), the attained compressed size (0.929,0.784, and 0.916), with RMSE (9.5,5.1, and 14.35) bpp, respectively. The main problem of the proposed system is the complexity of the compression and decompression algorithms, which led to a long execution time and suggested a lossy system compression that combines DCT and MMSA. The image is divided firstly into (non-fixed) blocks. Then, each block is exploited by the DCT. After that, each block is converted into a 1D vector, removing the zero values from the AC coefficients.

2. PROPOSED SYSTEM

This section involved the efficient lossy compression of grayscale images through the combined use of adaptive PBT and C321 techniques. The following steps discuss the proposed system in detail, and the layout of the proposed compression system is illustrated in **Fig. 1.**

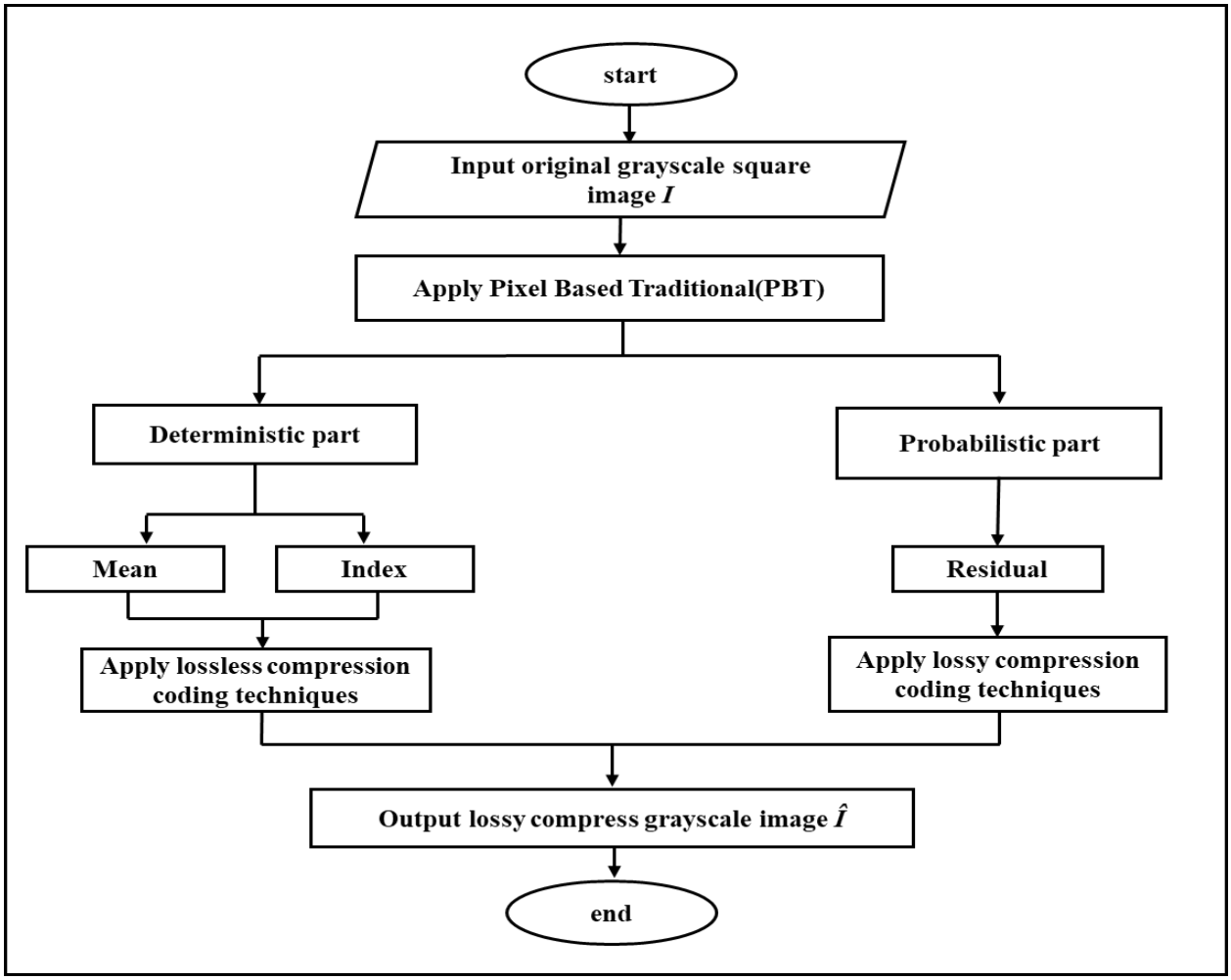

Figure 1. Flowchart of the proposed compression of adaptive PBT.

Step 1: Use input natural grayscale square image I of size N×N.
Step 2: Calculate the mean for each row in the image, read through the rows sequentially, and compute the average value for each row, as shown in Eq. (1) **(Hussain and Al-Khafaji, 2021)**.

$$Mean(m) = \frac{1}{n}\sum_{i}^{m} I(m,n) \quad (1)$$

For deterministic mean part (M) that encoded losslessly using the Double Differential Pulse Code Modulation (DDPCM) followed by arithmetic coding **(Salman, 2017)**.
Step 3: Select two control parameters: The initial input parameter is (limit), indicating the number of pixel neighbors. This parameter allows for the specification of how many Nvector values will be computed neighbors (limit). While the second parameter corresponds to the increment value between pixels (inc), this parameter allows for the specification of the distance (or difference) between two consecutive values of the Nvector.
Step 4: Create a vector of increment value (Vinc) by accumulating the value of inc, and the size of this vector depends on the limit value.
Step 5: For each value in the image row, calculate a neighbor vector multiplying (M) of the current row by each value in Vinc, according to Eq. (2) **(Hussain and Al-Khafaji, 2021)**.

$$Nvector(r) = floor(M \times Vinc(r) \quad (2)$$

where $Nvector$: neighbor vector of the current row, r is a positive value such that $1 \leq r \leq$ limit
To reconstruct (M) values losslessly using the inverse DDPCM (IDDPCM).

Step 6: Calculate the index ($Indx$) using Eq. (3) **(Hussain and Al-Khafaji, 2021)** and obtain the smallest positive value that is left over after a set of divisions between the current pixel value $I(m,n)$ and ($Nvector$) values of that row for every pixel in each row where this value should be positive.

$$Indx(m,t) = (I(m,n)/Nvector) \quad (3)$$

where $Indx$ is an array of indexes into the sub-mean value vector ($Nvector$) that yields the smallest remaining value using the BPS and C321 MMSA of three random logistic map keys generation, that explained using sub-steps below

i) Separate (isolate) the $Indx_{MSV}$ from $Indx_{LSV}$. According to Eq.s (4, 5) **(Sultan and George, 2021)**.

$$Indx_{MSV} = round(\frac{Indx}{Stp_{Indx}}) \quad (4)$$

$$Indx_{LSV} = Indx - (Indx_{MSV} \times Stp_{Indx}) \quad (5)$$

where $Indx$ is referred to as an index array ($Indx_{LSV}$ *and* $Indx_{MSV}$).
Stp_{Indx} is the value of the cut point bit. It is a very important parameter that partitions the values range.
The $Indx_{LSV}$ that encoded lossless using MMSA of C321 base of one-layer random logistic map key of three floating number base.

a) Create three random floating point keys of a one-layer scheme based on a logistic map according to Eq. (6).

$$\text{Key(i)} = mod(u \times xn \times (1 - xn), \max\ \_value) \quad (6)$$

where u control parameter or growth rate that directly affects random numbers generated **(Arif et al., 2022)**, xn refers to the initial value, and max $\_value$ maximum value of keys.

b) Convert $Indx_{LSV}$ into a vector, then create the *MMSA* of the *C321* base using Eq. (7).

$$MM_{LSV321}\ (i) = \sum_{t=m}^{M_s} \text{Key1} \times Indx_{LSV}(t) + \text{Key2} \times Indx_{LSV}(t+1) + \text{Key3} \times Indx_{LSV}(t+3) \quad (7)$$

where M_s corresponds to the size of $Indx_{LSV}$, and m=0, 3, 6, .9, …. is the compressed three values of *MMSA*, increased by three(represents each three data value into a single floating value by exploiting random key values between [0-1]), $Indx_{LSV}$ is the corresponding LSV of Indx and MM_{LSV321} is the compressed minimized matrix based on three data (the sum of the products of the weights and the original data values).

c) Preparing a Limited Space Search Table (LSST) containing $Indx_{LSV}$, a non-repeating, without redundancy to be used for decoding to prepare it for the sequential search algorithm, and preserve the value of the third parameter P(3) in a vector called SD to facilitate (speed up) the process of retrieval of data by searching for the first and second parameters only and Start with the last pointer, P(3), and increase it by one at each iteration, until reaching the last location (position) of LSST. Encode the *C321* parameters ($LSST, MM_{LSV321}, SD$) using dictionary-based techniques of *LZW and Huffman* base to acquire more compression performance.

ii) The $Indx_{MSV}$ that encoded losslessly using the BPS, where only the first layer of LSB is adopted (layer1). reconstruct ($Indx$) values losslessly using the inverse C321 for the $Indx_{LSV}$ according to Eq. (8), where the MMSA adopted here used third parameter P(3) in a vector called SD to facilitate (speed up) the data retrieval process by searching for only the first and second parameters instead of searching for three parameters, to make sure of efficiency and flexibility.

$$Rec\_MM_{IndxLSV321}\ (\text{i, j}) = \sum_{t=1}^{M_s} \text{K(t)} \times \text{LSST}\big(\text{P(t)}\big) + SD(t+2) \quad (8)$$

where Rec_MM_{LSV321} refer to $Indx_{LSV}$ reconstruct, LSST is Limited Space Search Table array, P refers to pointers, K refers to utilized Keys, Ms =3 represent the number of compressed values. On the other hand, the $Indx_{LSV}$ reconstructed. Finally, the index is reconstructed such as in:

$$Rec_{Indx} = (Indx_{MSV} \times Stp_{Indx}) + Indx_{LSV} \quad (9)$$

where:

Rec_{Indx} refers to the reconstructed index,
$Indx_{MSV}$ is MSV of the index,

and $Indx_{LSV}$ is LSV index. Stp_{Indx} is the value of the cut point bit that partitioned the values range.

Step 7: Compute the residual (Res) by finding the difference between the current pixel value, $I(m, n)$, and the selected nearest value (t) in the $Nvector$, as in Eq. (10).

$$Res(m,n) = I(m,n) - Nvector(r) \quad (10)$$

where:

Res is an array of reminder values (residual). If the current pixel value (r) is greater than any of the $Nvector$ values, save the value (r) in the *Indx* cell. (*Res*) encoded lossily starts by isolating the *Res* values into Res_{LSV} and Res_{MSV}, as in Eq.s (11 and 12) **(Sultan and George, 2021)**:

$$Res_{MSV} = round(\frac{Res}{Stp_{Res}}) \quad (11)$$

$$Res_{LSV} = Res - Res_{MSV} \times Stp_{Res} \quad (12)$$

where:

Res is the residual array,

Stp_{Res} is the value of the cut point bit, which is a very important parameter that partitions the values range.

Res_{MSV} compressed using the lossless MMSA of C321 base, according to Eq. (13).

$$MM_{MSV321}(i) = \sum_{t=m}^{M_s} \text{K(t)} \times Res_{MSV}(t) + \text{Key2} \times Res_{MSV}(t+1) + \text{Key3} \times Res_{MSV}(t+3) \quad (13)$$

where M_s corresponds to the size of Res_{MSV}, and m=0, 3, 6, .9, ... is the compressed three values of *MMSA* that increased by three, Res_{MSV} is the corresponding MSV part of a residual array, and MM_{MSV321} is the compressed minimized matrix based on three data (the sum of the products of the weights and the original data values). While Res_{LSV} utilized the DWT of two layers' decomposition scheme of Double Quantization Scheme (DQS) that mixed between the uniform base and hard thresholding base techniques for details subbands, according to Eq.s (14 to 17) **(Azman et al. 2019; Sadkhan, 2020; Narayana and Khan, 2020; Nandeesha and Somashekar, 2022):**

$$QRes_{LSV} = round(Res_{LSV} / Q_{Res}) \quad (14)$$

where Res_{LSV} is referred to as LSV of the residual array (*Res*), Q_{Res} represents the quantization step, and $QRes_{LSV}$ refers to the quantized Res_{LSV} uniformly.

$$H_{Res} = \begin{cases} LH_{(i,j)} & if\ |LH_{(i,j)}| \geq \text{Thr} \\ 0 & else \end{cases} \quad (15)$$

$$HL_{Res} = \begin{cases} HL_{(i,j)} & if\ |HL_{(i,j)}| \geq \text{Thr} \\ 0 & else \end{cases} \quad (16)$$

$$HH_{Res} = \begin{cases} HH_{(i,j)} & if\ |HH_{(i,j)}| \geq Thr \\ 0 & else \end{cases} \quad (17)$$

where LH_{Res} , HL_{Res} , and HH_{Res} are the quantized Res_{LSV} of hard base thresholding technique **(Zhang et al., 2019; Liu and Barber, 2020; Hagiwara, 2022)**, Thr corresponds to threshold value. To reconstruct lossily ($\hat{Res}$) using the inverse C321 base for Res_{MSV} along the inverse DWT of double quantization scheme of scalar and hard thresholding.

$$Rec_{Res} = (Res_{MSV} \times Stp_{Res}) + Res_{LSV} \quad (18)$$

Step 8: To reconstruct the original image, the sub-mean value of each row needs to be recalculated. This is because the decoding unit consists of three arrays (index, mean, and residual) that depend on the parameters (limit, inc), according to Eq.s (19 and 20).

$$R\_mean = Nvector(m) \times inc \times r \quad (19)$$

where r represents the lowest value in the residual array.

$$\hat{I}(m,n) = indx(m,n) \times inc + Rec_{Res}(m,n) \quad (20)$$

where Rec_{Res} is the inverse isolation (LSV&MSV) array of Res.

3. RESULTS AND DISCUSSION

The proposed system was implemented using MATLAB application version 2018b. This application is installed on a Laptop computer of Intel (R) Core(TM) i7-1065G7 CPU @ 1.30GHz 1.50 GHz, and Windows 10 Pro Operating system (64 bit). The system performance was tested/evaluated by adopting three standard grayscales (Lena.BMP, Male. TIF, and Woman dark hair. TIF) (256 gray levels or 8 bits/pixel) square (256×256) images of natural type from the Miscellaneous dataset. Generally, the popular and simple evaluation objective measures adopted by CR/ PSNR utilized according to Eq.s (21and 22) **(Abood, 2017; Al-Khafaji, 2018; Salih and Mahmood, 2018; Toama and Hussein, 2020).**

$$CR = \frac{OriginalSize\ in\ bytes}{Compressed\ size\ in\ bytes} \quad (21)$$

$$PSNR(\mathrm{I}, \hat{\mathrm{I}}) = 10log_{10}\left(\frac{255^2}{\frac{1}{N\times N}\sum_{i=0}^{N-1}\sum_{j=0}^{N-1}[\hat{\mathrm{I}}(i,j)-I(i,j)]^2}\right) \quad (22)$$

The proposed adaptive scheme utilizes a deterministic approach to exploit the DDPCM and a mixture of C321/bps techniques in a lossless manner for the mean (M) and index(Indx), respectively. Appropriate symbol encoder techniques follow this. The performance of the scheme is discussed below, including:

The first set of experiments is related to encoding M coefficients in the first deterministic part of the Adaptive PBT. These techniques utilize the DDPCM and an entropy encoder based on arithmetic coding **Table 1.** The effect of control parameters on the adaptive and traditional mean matrix for natural images in the (Miscellaneous) dataset compares the size in bytes for tested images using the proposed scheme with the Traditional PBT, which solely relies on probability-based techniques like DPCM/Huffman. The last column of the table

represents the savings in size according to Eq. (23), indicated as the difference between the two techniques.

$$SS = Original\ size\ in\ byte - Compressed\ size\ in\ byte \quad (23)$$

where SS is the Saving Size.

Table 1. A comparison of the tested images according to the mean size

Tested Images	Proposed Mean size (byte)	Traditional Mean size (byte)	SS(byte)
	DDPCM+ Arithmetic coding	DPCM+Huffman	
Lena	44	78	34
Male	55	89	34
Woman dark hair	39	90	51

The results presented in the table above clearly show the Adaptive techniques *SS* about (34-50) bytes, (39) bytes saving size on average for the proposed techniques compared to the traditional techniques, due to exploiting embedded spatial redundancy efficiently. When the number of neighbors(limit) is 10, and the value of the increase between these neighbors(inc) is 0.25. The second experiment related to the second deterministic part *Indx* of Adaptive PBT, that C321/BPS for LSV/ MSV losslessly along the entropy/dictionary encoders.
Table 2 presents the results of encoding *Indx* losslessly as a sum of $Indx_{MSV}$/ $Indx_{LSV}$ bytes. The range for the tested images in bytes is between(444 and 678). The control parameter u is set to 3.99 with an initial value of xn= 0.1 and a maximum value of 0.3. The comparison with the traditional techniques versus the proposed one shown in **Table 3** with SS exceeds (400) bytes on average to the selected tested image. The $CS_{Deterministic}$ size in bytes of three tested images, according to Eq. (24), is given in **Table 4.**

Table 2. Adaptive PBT of Indx for natural images in the (Miscellaneous) dataset.

Tested images	Case1: Limit= 10 , inc= 0.25, Stp= 10 u= 3.99 , max-value= 0.3, xn= 0.1		
	Size in byte of $Indx_{MSV}$	Size in byte of $Indx_{LSV}$	Indx ($Indx_{MSV}$ + $Indx_{LSV}$)
Lena	300	378	678
Male	292	352	644
Woman dark hair	200	244	444

Table 3. Comparison between traditional PBT and adaptive PBT of Index for natural images in the (Miscellaneous) dataset.

Tested images	Case1: Limit =10, inc=0.25 ,Stp=10 u=3.99 , max-value=0.3 ,xn=0.1		SS
	Proposed *Indx* size (byte)	Traditional *Index* size (byte)	
Lena	678	1276	598
Male	644	1088	444
Woman dark hair	444	792	348

Table 4. Size of a deterministic part after coding in the proposed system in bytes (Miscellaneous) for limit=10 & inc=0.25.

Tested images	M	$Index$	$CS_{Deterministic}$
Lena	44	678	722
Male	55	644	699
Woman dark hair	39	444	483

Table 5 shows a clear difference in the SS between $CS_{Deterministic}$ Proposed and $CS_{Deterministic}$ traditional.

$$CS_{Deterministic} = [Size\ byte\ of\ M + Size\ byte\ of\ Indx\ ] \quad (24)$$

Table 5. Comparison between $CS_{Deterministic}$ proposed and $CS_{Deterministic}$ traditional for natural images in the (Miscellaneous) dataset for limit=10 & inc= 0.25.

Tested image	$CS_{Deterministic}$ Proposed	$CS_{Deterministic}$ Traditional	SS
Lena	722	1354	632
Male	699	1177	478
Woman –dark hair	483	882	399

The third experiment is related to the residual image (*Res*) or probabilistic part, simply the difference between the original and best-predicted images. **Table 6** shows three tested images experimenting with several values of Thr_{Res} ranging between (0.3, 1.2, and 2.3), where Thr_{Res} has a direct effect on $Res_{LSV,}$ which is the saving size in bytes SS, in addition to using three cases of Q (2-5), that also has a role in reducing the size of *Res*.

Table 6. Adaptive PBT of Res_{LSV} & Res_{MSV} for natural images in the (Miscellaneous) dataset.

Tested images	Thr_{Res}	Case1: limit= 10, inc=0.25, STP_{Res}=10			
		Res_{LSV}			Res_{MSV}
		Q= 2	Q= 4	Q= 5	
Lena	0.3	3614	2508	2274	3080
	1.2	1700	1362	1090	
	2.3	768	610	544	
Male	0.3	3570	2504	2270	3088
	1.2	1662	1344	1098	
	2.3	772	618	558	
Woman dark hair	0.3	3474	2424	2212	3034
	1.2	1686	1266	1148	
	2.3	838	674	606	

The *Res* coded lossily using the Res_{LSV} and Res_{MSV} separation base. The former utilized the Haar DWT two-layer decomposition scheme along hard thresholding (the threshold value selection determines which coefficients are kept and which ones are discarded, thus influencing both the compression ratio and the quality of the reconstructed data). At the same time, the latter exploited the C321 of three key bases.

The fourth experiment evaluates the performance of the adaptive PBT by measuring the CR using Eq. (21) and the quality in terms of PSNR based on Eq. (22), as given in **Table 7**. The evaluation measure in the former implicitly requires the size of the compressed image data information, which is the sum of the deterministic and probabilistic parts.

Table 7. Proposed compression system performance for the tested images (Miscellaneous) dataset for APBT with Limit= 10 & inc= 0.25.

Tested images	$CS_{Deterministic}$	Q	Thr_{Res}	$CS_{probabilistic}$	$Comp_{PBT}$	CR	PSNR
Lena	722	2	0.3	6694	7416	9.3743	51.0307
		4	1.2	4442	5164	14.1914	44.1232
		5	2.3	3624	4346	18.0839	40.5010
Male	741	2	0.3	6658	7399	8.8574	50.9958
		4	1.2	4432	5173	12.6689	44.1970
		5	2.3	3646	4387	14.9387	40.5962
Woman dark hair	483	2	0.3	6508	6991	10.0701	53.7642
		4	1.2	4300	4783	15.2409	48.5589
		5	2.3	3640	4123	18.0044	45.1912

Generally, this *Res* part exhausted a large number of bytes due to the limitation or restriction of utilizing a fixed probabilistic model since image details vary with fixed/nonadaptive modeling. In contrast, the traditional PBT adopted the hierarchal quantization scheme, which nearly used about 50% of compressed image information on average, as shown in **Table 8**. Hence, the proposed adaptive base techniques aim to overcome this obstacle.

Table 8. Comparison between traditional PBT and adaptive PBT of residual (Res) with Q= 4 and Thr_{Res}= 1.2 for natural images in the (Miscellaneous) dataset

Tested images	Case1: limit: 10, inc: 0.25		SS
	$CS_{Probablistic}$ Proposed (Res_{MSV}+Res_{LSV}) size (byte)	$CS_{Probablistic}$ Traditional Res size (byte)	
Lena	4442	10132	5690
Male	4432	10383	5951
Woman dark hair	4300	9054	4754

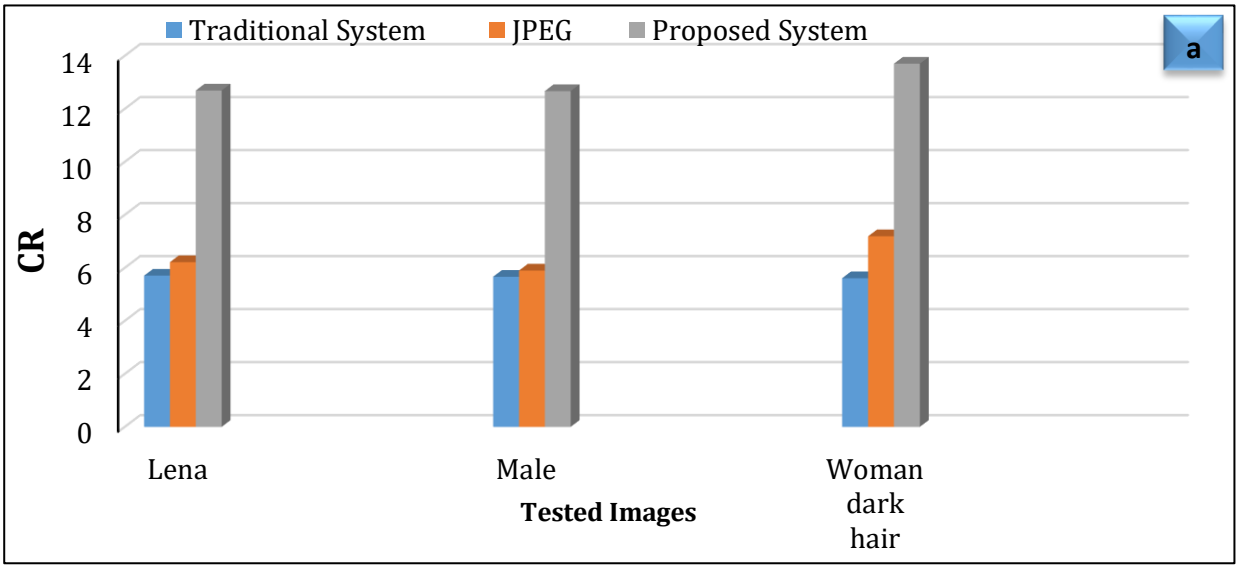

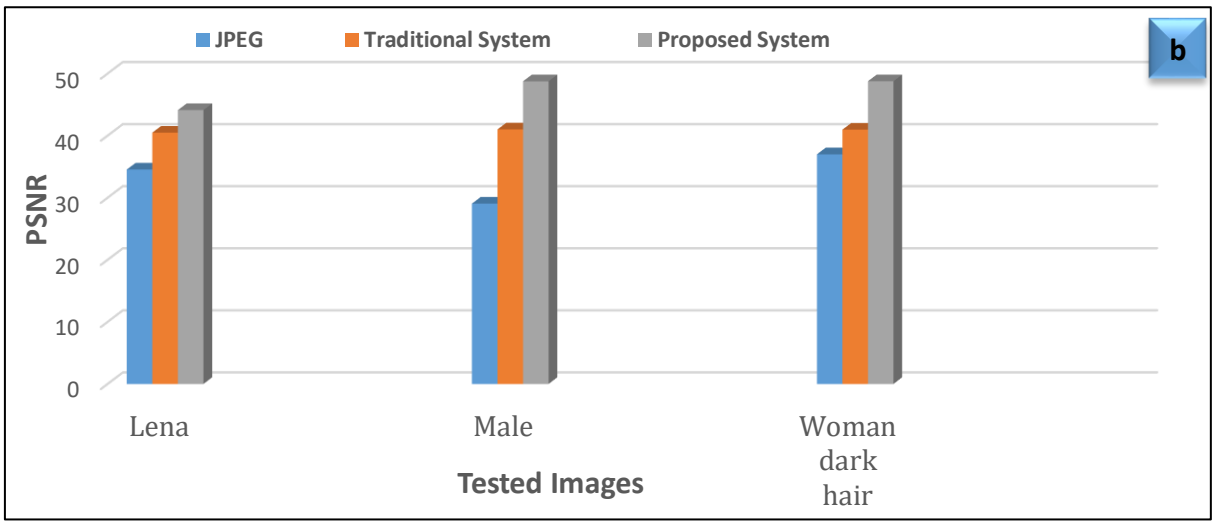

Figure 2. Comparison between traditional PBT and adaptive PBT of (a) CR (Miscellaneous) data and (b) PSNR (Miscellaneous) data

Finally, the experiment compares the proposed compression system of adaptive PBT with traditional PBT and commonly used standard image compression techniques such as JPEG. The results shown in **Table 9** and **Fig. 2** imply less reduction in compressed adaptive PBT information than traditional PBT when SS exceeds 5000 bytes, which is nearly 50%. This difference can be attributed to the utilization of various technologies. The results demonstrate that adaptive PBT performs highly in CR of 13 and PSNR of 48 dB.

Table 9. Comparison of standard JPEG with traditional PBT and adaptive PBT for natural images in the (Miscellaneous) dataset regarding the system total size, CR, and PSNR.

Tested images	Proposed System limit=10, inc=0.25 Q= 4, Stp= 10, Thr_{Res}= 1.2			Traditional System limit= 10, inc= 0.25 Q= 20, a = 1.3 b= 1.6			JPEG		
	Size in Byte	CR	PSNR	Size in Byte	CR	PSNR	Size in Byte	CR	PSNR
Lena	5164	12.6909	44.1232	10547	5.7057	40.4866	11059	5.9260	34.7484
Male	5186	12.6689	48.7577	11264	5.6648	41.0053	10342	6.3368	35.5745
Woman dark hair	4748	13.7019	48.7641	11681	5.6105	40.9739	9113	7.1910	36.9966

4. CONCLUSIONS

This study aimed to construct an efficient grayscale image compression system with an increased reduction in storage capacity for natural base images. The adaptive PBT, used as a lossy hybrid compression system, encodes the pixel-based modeling scheme of the deterministic part (mean, index) and the probabilistic amount (residual) using various techniques such as DPCM, BPS, and C321 of MMSA, which is based on three lossless values in a sequential search scheme with three keys derived from the logistic map. These keys play a role in reducing the size and achieving higher compression ratios compared to the

traditional approach. Additionally, SD speeds up the encoding and decoding processes. The results demonstrate that the proposed system exhibits superior compression efficiency and image quality compared to the traditional PBT system and the standard JPEG. The proposed approach achieves a CR of 12 to 13 and a PSNR of 44 to 48 dB.
In contrast, the traditional PBT system achieves a CR of 5, with a PSNR between 40 and 41 dB. Additionally, compared to JPEG, the adaptive PBT system outperforms with a CR ranging from 5 to 7 and a PSNR ranging from 34 to 36 dB. However, the proposed system still has limitations in extending the system to color images of square/non-square dimensions and using non-uniform quantization with MMSA of C321. Further comparison of the results and using a multi-layer/integer key-generated technique are recommended.

NOMENCLATURE

Symbol	Description	Symbol	Description
CR	Compression Ratio	PSNR	Peak Signal to Noise Ratio
K	Key	Q	Quantization step
$\hat{I}(m,n)$	reconstruct the original image	r	Positive value
$indx_{Lsv}$	Least Significant value of Indx	Rec_{Indx}	The index reconstructed
$indx_{Msv}$	Most Significant value of Indx	Rec_MM_{LS}	The LSV of index reconstructed
inc	Increment value	Res	Array of reminder values (residual)
Indx	array of indexes	Res_{LSV}	Least Significant value of Res
limit	Number of neighbour	Res_{MSV}	Most Significant value of Res
LSST	Limited Space Search Table array	Rec_{Res}	The Res reconstructed
LH_{Res}, HL_{Res}, and HH_{Res}	The quantized Res_{LSV} of hard base thresholding	SS	Saving size
M	Mean array	SD	Support Data
m,n	Size of image	Stp	Value of the cut point bit
MM_{MSV321}	Minimized matrix based on three data	t	Three values of MMSA
max-value	Maximum value of keys	Thr	Threshold value
M_s	The size of $Indx_{LSV}$	u	Control parameter
Nvector	Sub-mean value vector	Vinc	Accumulating the value of inc
p	Pointer	xn	Initial value

Acknowledgements

This work was supported by the University of Baghdad. We also wish to thank the anonymous reviewers for their comments and suggestions, which helped enhance the quality of the paper

Credit Authorship Contribution Statement

Zahraa.H. Abed: Writing – review and editing, Writing – original draft, Validation, Software, Methodology.. Ghadah K. AL-Khafaji: Validation, Software, Methodology.

Declaration of Competing Interest

The authors declare that they have no known competing financial interests or personal relationships that could have appeared to influence the work reported in this paper.

REFERENCES

Abed, Z.H., and AL-Khafaji, G.K., 2022. Pixel based techniques for gray image compression: A review. *Journal of Al-Qadisiyah for Computer Science and Mathematics*, 14(2), pp. 59–70. Doi:10.29304/jqcm.2022.14.2.967.

Abood, Z.I., 2017. Composite techniques based color image compression. *Journal of Engineering*, *23*(3), pp. 80-93. Doi:10.31026/j.eng.2017.03.06.

Abood, Z.I., 2013. Image compression using 3-D two-level techniques. *Journal of Engineering*, 19(11), pp. 1407-1424. Doi:10.31026/j.eng.2013.11.05.

Ahmed, R.H., and Hamza, E.K., 2021. Designing a Secure Software-Defined Radio Transceiver using the Logistic Map. *Journal of Engineering*, 27(6), pp. 59–72. Doi:10.31026/j.eng.2021.06.05.

Ahmed, Z J., George, L.E., and Abduljabbar, Z.S., 2020. Fractal image compression using block indexing technique: A review. *Iraqi Journal of Science,* 61(7), pp.1798-1810. Doi:10.24996/ijs.2021.62.

Ahmed, Z.J., George, L.E., and Hadi, R.A., 2021. Audio compression using transforms and high order entropy encoding. *International Journal of Electrical and Computer Engineering*, 11(4), pp. 3459–3469. Doi:10.11591/ijece.v11i4.pp3459-3469.

Al-hadithy, S.S., Al-khafaji, G.K., and Siddeq, M.M., 2021. Adaptive 1-D Polynomial Coding of C621 Base for Image Compression, *Turkish Journal of Computer and Mathematics Education (TURCOMAT)*, 12(13), pp. 5720-5731.

AL-Hadithy, S.S., and AL-Khafaji, G.K., 2022. Adaptive 1-D polynomial coding to compress color image with C421. *International Journal of Nonlinear Analysis and Applications*. pp. 1261–1276. Doi:10.22075/ijnaa.2022.7013.

Al-Khafaji, G., and Fadhil, S., 2017. Image Compression based on Fixed Predictor Multiresolution Thresholding of Linear Polynomial Near lossless Techniques. *Journal of Al-Qadisiyah for computer science and mathematics*, *9*(2), P. 35. Doi:10.29304/jqcm.2017.9.2.bit

Al-Khafaji, G.K., 2018. Linear Polynomial Coding with Midtread Adaptive Quantizer. *Iraqi Journal of Science*, *59*(1c), pp. 585-590. Doi: 10.24996/IJS.2018.59.1C.15.

Al-Khafaji, G.K., and Gorrge, L.E., 2021. Grey-level image compression using 1-d polynomial and hybrid encoding techniques. *Journal of Engineering Science and Technology*, 16(6), pp. 4707–4728.

AL-Khafaji, G.K., Rasheed, M.H., Siddeq, M.M., and Rodrigues, M.A., 2023. Adaptive polynomial coding of multi-base hybrid compression. *International Journal of Engineering*, 36(2), pp. 236–252. Doi:10.5829/ije.2023.36.02b.05.

Abd-Alzhra, A.S., and Al-Tamimi, M.S., 2021. Lossy image compression using hybrid deep learning autoencoder based on k-mean clustering. *International Journal of Intelligent Engineering & Systems*, pp. 7848-7861.

Abd-Alzhra, A. S., and Al- Tamimi, M. S. H., 2022. Image compression using deep learning: methods and techniques. *Iraqi Journal of Science*, 63(3), pp. 1299–1312. Doi:10.24996/ijs.2022.63.3.34.

Abu-Faraj, M.A., Al-Hyari, A., Obimbo, C., Aldebei, K., Altaharwa, I., Alqadi, Z., and Almanaseer, O., 2023. Protecting digital images using keys enhanced by 2D chaotic logistic maps. *Cryptography*, *7*(2), pp.1-20. Doi:10.3390/cryptography7020020.

Arif, J., Khan, M. A., Ghaleb, B., Ahmad, J., Munir, A., Rashid, U., and Al-Dubai, A. Y., 2022. A novel chaotic permutation-substitution image encryption scheme based on logistic map and random substitution. *IEEE Access*, 10, pp. 12966-12982. Doi:10.1109/access.2022.3146792.

Azman, N.A.N., Ali, S., Rashid, R.A., Saparudin, F.A., and Sarijari, M.A., 2019. A hybrid predictive technique for lossless image compression. *Bulletin of Electrical Engineering and Informatics*, 8(4), pp. 1289-1296. Doi: 10.11591/eei.v8i4.1612.

Chuman, T., Iida, K. and Kiya, H., 2017, December. Image manipulation on social media for encryption-then-compression systems. *2017 Asia-Pacific Signal and Information Processing Association Annual Summit and Conference (APSIPA ASC)* (pp. 858-863). IEEE. Doi:10.1109/APSIPA.2017.8282153 .

George, LE., Hassan, E.K., Mohammed, S.G., and Mohammed, F.G., 2020. Selective image encryption based on DCT, hybrid shift coding and randomly generated secret key. *Iraqi Journal of Science*, pp.920-935. Doi: 10.24996/ijs.2020.61.4.25.

Hagiwara, K., 2022. Bridging between soft and hard thresholding by scaling. *IEICE TRANSACTIONS on Information and Systems*, *105*(9), pp.1529-1536. Doi: 10.1587/transinf.2021EDP7223.

Hussain, A.A., and AL-Khafaji, G.K., 2021. A pixel based method for image compression. *Tikrit Journal of Pure Science*, 26(1), pp. 1813-1662. Doi:10.25130/tjps.v26i1.108.

Hussain, A.A., Al-Khafaji, G.K., and Siddeq, M.M., 2020. Developed JPEG Algorithm Applied in Image Compression, *IOP Conference Series: Materials Science and Engineering*, 928(3). Doi:10.1088/1757-899X/928/3/032006.

Hussain, A.J., Al-Fayadh, A., and Radi, N., 2018. Image compression techniques: A survey in lossless and lossy algorithms. *Neurocomputing*, 300, pp. 44–69. Doi: 10.1016/j.neucom.2018.02.094.

Ibrahim, A.A., George, L.E., and Hassan, E.K., 2020. Color image compression system by using block categorization based on spatial details and DCT followed by improved entropy encoder. *Iraqi Journal of Science*, 61(11), pp. 3127–3140. Doi:10.24996/ijs.2020.61.11.32.

Liu, X., An, P., Chen, Y., and Huang, X., 2022. An improved lossless image compression algorithm based on Huffman coding. *Multimedia Tools and Applications*, 81(4), pp. 4781–4795. Doi:10.1007/s11042-021-11017-5.

Kabir, M.A., and Mondal, M.R.H., 2018. Edge-based and prediction-based transformations for lossless image compression. *Journal of Imaging*, *4*(5), P.64. Doi: 10.3390/jimaging4050064.

Liu, H., and Foygel Barber, R., 2020. Between hard and soft thresholding: optimal iterative thresholding algorithms. *Information and Inference: A Journal of the IMA*, 9(4), pp. 899-933. Doi:10.1093/imaiai/iaz027.

Maghari, A., 2019. A comparative study of DCT and DWT image compression techniques combined with Huffman coding. *Jordanian Journal of Computers and Information Technology*, *5*(2). Doi:10.5455/jjcit.71-1554982934

Mohammed, S.G., Abdul-Jabbar, S.S., and Mohammed, F.G., 2021, December. Art Image Compression Based on Lossless LZW Hashing Ciphering Algorithm. *Journal of Physics: Conference Series*, 2114(1), p. 012080. Doi:10.1088/1742-6596/2114/1/012080.

Gashnikov, M., and Maksimov, A., 2018, August. Parameterized four direction contour-invariant extrapolator for DPCM image compression. In *Tenth International Conference on Digital Image Processing (ICDIP 2018)*,10806, pp. 1229-1238. Doi:10.1117/12.2503003.

Mahdi, N.S., and Al-Khafaji, G.K., 2022. Image compression using polynomial coding techniques: A review. *Journal of Al-Qadisiyah for Computer Science and Mathematics*, 14(2), pp. 70-81. Doi:10.29304/jqcm.2022.14.2.968

Nandeesha, R., and Somashekar, K., 2023. Content-Based Image Compression Using Hybrid Discrete Wavelet Transform with Block Vector Quantization. *International Journal of Intelligent Systems and Applications in Engineering*, *11*(5s), pp.19-37.

Narayana, P.S., and Khan, A.M., 2020. MRI image compression using multiple wavelets at different levels of discrete wavelets transform. *Journal of Physics: Conference Series*,1427(1), P. 012002. Doi:01200/1/1427/6596-1742/10.1088.2.

Rafea, S., and Salman, N.H., 2018. Hybrid DWT-DCT compression algorithm & a new flipping block with an adaptive RLE method for high medical image compression ratio. *International Journal of Engineering & Technology*, *7*(4), pp. 4602-4606. Doi: 10.14419/ijet.v7i4.25904.

Rasheed, M.H., Salih, O.M., Siddeq, M.M., and Rodrigues, M.A., 2020. Image compression based on 2D discrete Fourier transform and matrix minimization algorithm. *Array*, 6, P. 100024. Doi:10.1016/j.array.2020.100024.

Sadkhan, S.B., 2020, September. A proposed image compression technique based on DWT and predictive techniques. *In 2020 3rd International Conference on Engineering Technology and its Applications (IICETA),* pp. 246-251. IEEE. Doi:10.1109/IICETA50496.2020.9318802

Salih, A.M., and Mahmood, S.H., 2019. Digital color image watermarking using encoded frequent mark. *Journal of Engineering*, *25*(3), pp. 81-88. Doi:10.31026/j.eng.2019.03.07.

Salman, N.H., and Rafea, S., 2020. The arithmetic coding and hybrid discrete wavelet and cosine transform approaches in image compression. *Journal of Southwest Jiaotong University*, 55(1), pp. 1–9. Doi: 10.35741/issn.0258-2724.55.1.6.

Salman, N.H., 2021. Compare arithmetic coding to the wavelet approaches for medical image compression. *Journal of Engineering Science and Technology*, *16*(1), pp. 737-749.

Salman, N., 2017. New image compression/decompression technique using arithmetic coding algorithm. *Journal of Zankoy Sulaimani*, *19*(1), pp. 263-272. Doi:10.17656/18124100.

Shihab, H.S., 2023. Image compression techniques on-Board small satellites. *Iraqi Journal of Science*, 64(3), pp. 1518-1534. Doi:10.24996/ijs.2023.64.3.40.

Siddeq, M.M., and Al-Khafaji, G.K., 2013. Applied minimized matrix size algorithm on the transformed images by DCT and DWT used for image compression. *International Journal of Computer Applications*, 70(15). pp. 33-40. Doi:10.5120/12040-8000.

Siddeq, M.M., and Rodrigues, M.A., 2015. A Novel 2D Image Compression Algorithm Based on Two Levels DWT and DCT Transforms with Enhanced Minimize-Matrix-Size Algorithm for High Resolution Structured Light 3D Surface Reconstruction .*3D Research*. 6(3), pp. 1–35. Doi:10.1007/s13319-015-0055-6.

Siddeq, M.M., and Rodrigues, M.A., 2017. A novel high-frequency encoding algorithm for image compression. *EURASIP Journal on Advances in Signal Processing*, 2017, pp. 1-17. Doi:10.1186/s13634-017-0461-4.

Sultan, B.A., and George, L.E., 2021. Color image compression based on spatial and magnitude signal decomposition. *International Journal of Electrical and Computer Engineering (IJECE)*, 11(5), pp. 4069-4081. Doi:10.11591/ijece.v11i5.pp4069-4081.

Toama, R.J., and Hussein, M.N., 2020. A secure cipher for the gray images based on the shamir secret sharing scheme with discrete wavelet haar transform. *Journal Of Mechanics Of Continua And Mathematical Sciences*, 15(6), pp. 334-351. Doi:10.26782/jmcms.2020.06.00025.

Yousif, R.I., and Salman, N.H., 2021. Image compression based on arithmetic coding algorithm. *Iraqi Journal of Science*, 62(1), pp. 329–334. Doi:10.24996/ijs.2021.62.1.31.

Zhang, Y., Ding, W., Pan, Z., and Qin, J., 2019. Improved wavelet threshold for image de-noising. *Frontiers in neuroscience*, *13*, P. 39. Doi: 10.3389/fnins.2019.00039.